

GENERAL MECHANICS

FULL DYNAMIC REACTIONS IN THE BASIC SHAFT BEARINGS OF BIG BAND SAW MACHINES

BOYCHO MARINOV

*Institute of Mechanics, Bulgarian Academy of Sciences,
Acad. G. Bonchev St., Bl. 4, 1113 Sofia, Bulgaria,*

e-mails: boicho_marinoff@yahoo.co.uk, boicho_marinoff@abv.bg

[Received 03 September 2012. Accepted 05 November 2012]

ABSTRACT. The band saws machines are a certain class woodworking machines for longitudinal or transversal cutting as well as for curvilinear wood cutting. These machines saw the wood through a band-saw blade and two feeding wheels. These wheels usually are very large and they are produced with inaccuracies. The centre of mass of the disc is displaced from the axis of rotation of the distance e (eccentricity) and the axis of the disk makes an angle α with the axis of rotation. In this paper, the dynamic reactions in the bearings of the basic shaft, which drives the band saw machines, are analyzed. These reactions are caused by the external loading and the kinematics and the mass characteristics of the rotating disk. The expressions for the full dynamic reactions are obtained. These expressions allow the parameters of the machines to be chosen in such a way that the loading in the shaft and the bearings to be minimal.

KEY WORDS: Band saw machines, basic shafts, band-saw blade, feeding wheels, belt pulleys, bearings, kinematics and mass characteristics, dynamic reactions.

1. Introduction

The band saws are a certain class woodworking machines for longitudinal or transversal cutting as well as for curvilinear wood cutting. They are used for cutting of boards, slabs, prisms, details etc. They saw the wood through a band-saw blade and two feeding wheels. The lower feeding wheel is a driving one. It is driven through the electric motor and the belt transmission. The cutting part of the band-saw blade is the rectilinear part. It performs uniform motion. The cutting velocity has constant value and it is the vertical one. The feeding mechanism performs detail translational motion with a constant velocity. This velocity is perpendicular to the cutting one.

The two feeding wheels usually are very large and they are manufactured with inaccuracies. The centre of mass of the disc is displaced from the axis of rotation of the distance e (eccentricity) and the axis of the disk makes an angle α with the axis of rotation. In this paper, the dynamic reactions in the bearings of the basic shaft, which drives the band saw machines, are analyzed. These reactions are caused by the external loading and the kinematics and mass characteristics of the rotating disk. The expressions for the full dynamic reactions are obtained. These expressions allow the parameters of the machines to be chosen in such a way that the loading in the shaft and the bearings to be minimal.

2. Expose

2.1. Principle Scheme of the Band Saw Machine

Figure 1 shows scheme of the band saws [1, 2, 3, 4, 5]. We define the following symbols: 1, 2, 5, 6 – belt pulleys, E – electric motor, 3 and 4 – feeding wheels, A – band-saw blade, 7 and 8 – chain-wheels.

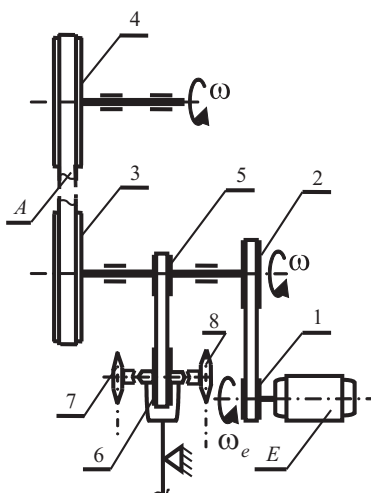


Fig. 1. Principle scheme of band saw

2.2. Dynamic Model

The dynamic model, shown in Fig. 2 is used for solving the problems. The feeding wheel 3 and the belt pulleys 2 and 5 perform rotation with a constant angular velocity ω about the axis of rotation AB . In this case, the mechanical system (the feeding wheel, the belt pulleys and the basic shaft) describes an angle $\varphi = \omega t$.

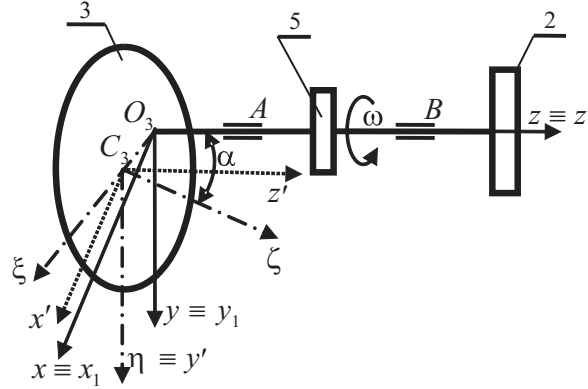


Fig. 2. Dynamic model

We choose the following coordinate systems: Fixed coordinate system O_3xyz , moving coordinate system $O_3x_1y_1z_1$, which moves along with the feeding wheel. In the initial moment ($\varphi = 0$), the axes of the two coordinate systems coincide. Coordinate system $C_3x'y'z'$ begins at the centre of mass C_3 . Its axes are parallel to the axes of the moving coordinate system. We use fourth coordinate system $C_3\xi\eta\zeta$. The axes of this coordinate system are the principal axes of inertia of the disk. The centre of mass C_3 of the feeding wheel 3 is displaced from the axis of rotation $AB \equiv z \equiv z_1$ of an eccentricity $e = O_3C_3$ and circumscribe circle with a radius $\rho_{C_3} = e \cos \alpha$ around this axis. The axis $C_3\zeta$ of the disk makes an angle α with the rotation axis.

2.3. Dynamic Reactions as a Consequence of the External Loading

We consider separately the forces that load up the feeding wheel 3 and belt pulleys 2 and 5.

2.3.1. Feeding Wheel

The feeding wheel 3 is shown in Fig. 3. The forces that load up the wheel are shown also. The tangential force P_3^e is equal to the cutting force P_b^r , i.e. $P_3^e = P_b^r$. This force is calculated from the next dependence [1, 2]:

$$(1) \quad P_b^r = \frac{K_{\Delta(\lambda)} b H u}{V},$$

where V is the cutting velocity [m/s], H is the thickness of the working detail [m], u is the feeding velocity [m/s], b is the width of the cutter [m], $K_{\Delta(\lambda)}$ [J/m³] is the specific work of the cutting. It is determined from the expressions

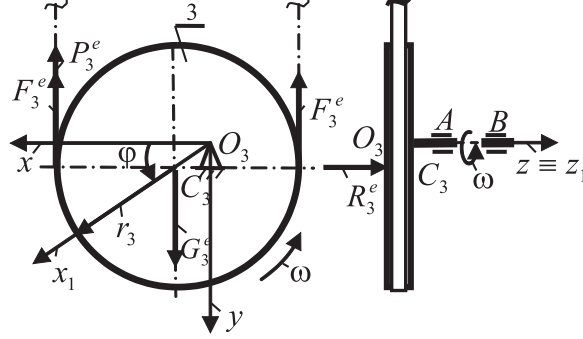


Fig. 3. Feeding wheel

below [1,2]:

$$(2) \quad K_{\Delta} = k + \frac{\alpha_{\rho} p_3}{u_z} + \frac{\alpha_{\Delta} H}{b}, \quad K_{\lambda} = k + \frac{\alpha_{\rho} p_3 s}{u_z \cdot b} + \frac{\alpha_{\lambda} H}{b}.$$

In the expressions (2) the next symbols are used: The index (Δ) is used for flattened teeth, the index (λ) is used for teeth setting, k is a fictitious pressure on the front side of the teeth [N/m^2], p_3 is a fictitious specific force on the back side of the teeth [N/m], α_{ρ} is a coefficient of the blunt teeth, s is a thickness of the band-saw blade [m], u_z is feed of one tooth. The friction intensity of the shavings on the cutting walls is marked with α_{Δ} and α_{λ} like $\alpha_{\Delta} = 196 \cdot 10^3$ [Pa], $\alpha_{\lambda} = 1,25\alpha_{\Delta}$, [1, 3].

The tangential force P_3^e creates moment of resistance M_{3z}^e with respect to the axis of rotation, which is calculated by the following dependence:

$$(3) \quad M_{3z}^e = P_3^e (r_3 + e \cos \varphi) = \frac{K_{\Delta(\lambda)} b H u}{V} (r_3 + e \cos \omega t).$$

The forces F_3^e are the tensile forces in the band-saw blade. R_3^e is the force that loads the wheel 3. It is calculated by the following expression:

$$(4) \quad R_3^e = \frac{1}{2} P_u = \frac{R_b^n + R_{\Sigma}}{2},$$

where P_u is the feeding force, R_b^n is the normal force with which the band-saw blade loads up the detail. This force has the following relation with respect to the force P_b^r :

$$(5) \quad R_b^n = m P_b^r,$$

where m is a coefficient, dependent on the state of the band-saw blade ($m = 0.5$ for a sharp band-saw blade and $m = 1$ for a very blunt band-saw blade). R_{Σ} is the total resistance force on the woodworking detail. This force is calculated for each individual case. Figure 4 shows the woodworking detail and the forces and the velocities described above.

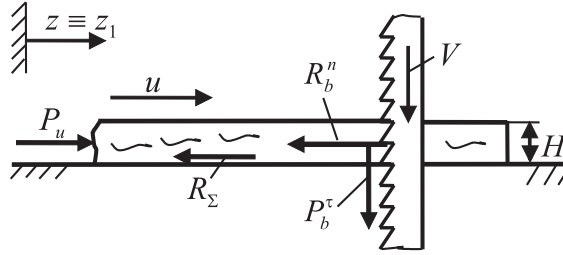


Fig. 4. Working detail and the band-saw blade

The weight of the feeding wheel 3 is:

$$(6) \quad G_3^e = m_3 g,$$

where m_3 is its mass and g is the acceleration of gravity.

2.3.2. Belt Pulley 2

The belt pulley position 2 is shown in Fig. 5, below:

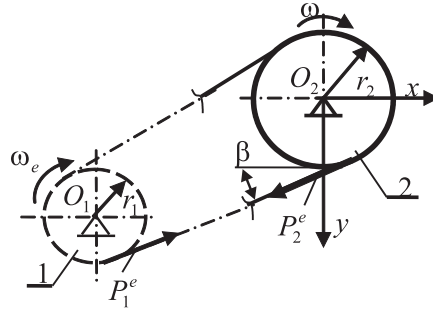


Fig. 5. Belt pulley – position 2

This belt pulley transmits the driving moment from the electric motor to the basic shaft. The force P_2^e creates the driving moment M_{2z}^e with respect to the axis of rotation. It is calculated from the known expression, cited below:

$$(7) \quad M_{2z}^e = P_2^e r_2.$$

This force is equal to the force P_1^e in the belt gear. The electric motor creates a moment which can be calculated from the following expression:

$$(8) \quad M_1^e = N_e / \omega_e,$$

where N_e is the power of the electric motor for cutting and feeding of the woodworking detail, ω_e is the angular velocity of the electric motor. This moment is equal to the moment, created by the force P_1^e .

$$(9) \quad M_1^e = P_1^e r_1.$$

We obtain the final correlation between the forces P_1^e and P_2^e .

$$(10) \quad P_1^e = P_2^e = \frac{N_e}{\omega_e r_1}.$$

We replace the above expression in the expression (7) and we obtain final expression for the moment M_{2z}^e .

$$(11) \quad M_{2z}^e = i_{12} \frac{N_e}{\omega_e},$$

where $i_{12} = r_2/r_1$ is the gear ratio. The tensile forces in the belt and the weight of the washer are not taken into account.

2.3.3. Belt Pulley 5

The belt pulley - position 5 is shown in Fig. 6. This pulley drives the feeding mechanism.

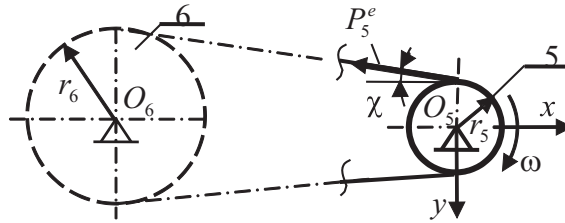


Fig. 6. Belt pulley – position 5

The force P_5^e creates a moment of resistance M_{5z}^e . This moment is calculated from the following expression:

$$(12) \quad M_{5z}^e = P_5^e r_5.$$

The moments of the weight G_3^e with respect to the coordinate axes are calculated by the following dependencies:

$$(18) \quad \begin{aligned} M_{G_{3x}}^e &= G_3^e e \sin \alpha = m_3 g e \sin \alpha, \\ M_{G_{3y}}^e &= 0, \\ M_{G_{3z}}^e &= G_3^e e \cos \alpha \cos \varphi = m_3 g e \cos \alpha \cos \omega t. \end{aligned}$$

The force P_{3y}^e is calculated from the dependence below:

$$(19) \quad P_{3y}^e = 2F_3^e + P_3^e = 2F_3^e + \frac{K_{\Delta(\lambda)} b H u}{V}.$$

The components P_{2x}^e and P_{2y}^e of the force P_2^e shown in Fig. 5, are determined by the dependencies below:

$$(20) \quad P_{2x}^e = P_2^e \cos \beta = \frac{N_e \cos \beta}{\omega r_2}, \quad P_{2y}^e = P_2^e \sin \beta = \frac{N_e \sin \beta}{\omega r_2}.$$

The components P_{5x}^e and P_{5y}^e of the force P_5^e shown in Fig. 6, are determined by the following relations:

$$(21) \quad P_{5x}^e = P_5^e \cos \chi = \frac{P_u u \cos \chi}{\omega r_5}, \quad P_{5y}^e = P_5^e \sin \chi = \frac{P_u u \sin \chi}{\omega r_5}.$$

The support reactions are determined by the equilibrium conditions.

$$(22) \quad \sum z_i = 0, \quad \sum M_{Axi} = 0, \quad \sum M_{Bxi} = 0, \quad \sum M_{Ayi} = 0, \quad \sum M_{Byi} = 0.$$

We write equations (22) as follows:

$$(23) \quad \begin{aligned} R_{3z}^e - A_z^e &= 0, \\ M_{R_{3x}}^e + M_{G_{3x}}^e + (G_3^e - P_{3y}^e) a_1 + P_{5y}^e b_1 - B_y^e (b_1 + c_1) &= 0, \\ -P_{2y}^e (b_1 + c_1 + d_1) &= 0, \\ M_{R_{3x}}^e + M_{G_{3x}}^e + (G_3^e - P_{3y}^e) (a_1 + b_1 + c_1) + A_y^e (b_1 + c_1) &= 0, \\ -P_{5y}^e c_1 - P_{2y}^e d_1 &= 0, \\ -M_{R_{3y}}^e - P_{5x}^e b_1 + B_x^e (b_1 + c_1) - P_{2x}^e (b_1 + c_1 + d_1) &= 0, \\ -M_{R_{3y}}^e - A_x^e (b_1 + c_1) + P_{5x}^e c_1 - P_{2x}^e d_1 &= 0. \end{aligned}$$

We get the final expressions for the support reactions.

$$(24) \quad \begin{aligned} A_z^e &= \frac{\cos \alpha}{2} \left(\frac{mK_{\Delta(\lambda)}bHu}{V} + R_{\Sigma} \right), \\ B_y^e &= L_1 e \cos \alpha \sin \omega t + L_2 e \sin \alpha + L_3, \\ A_y^e &= M_1 e \cos \alpha \sin \omega t + M_2 e \sin \alpha + M_3, \\ B_x^e &= N_1 e \cos \alpha \cos \omega t + N_2 \cos \alpha + N_3, \\ A_x^e &= S_1 e \cos \alpha \cos \omega t + S_2 \cos \alpha + S_3. \end{aligned}$$

The following substitutions are performed in the above expressions:

$$\begin{aligned} L_1 &= \frac{1}{2(b_1 + c_1)} \left(\frac{mK_{\Delta(\lambda)}bHu}{V} + R_{\Sigma} \right), & L_2 &= \frac{m_3g}{(b_1 + c_1)}, \\ L_3 &= \left(m_3g - 2F_3^e - \frac{K_{\Delta(\lambda)}bHu}{V} \right) \frac{a_1}{(b_1 + c_1)} \\ &\quad + \frac{P_u u b_1 \sin \chi}{\omega r_5 (b_1 + c_1)} - \frac{N_e (b_1 + c_1 + d_1) \sin \beta}{\omega r_2 (b_1 + c_1)}, \\ M_1 &= -\frac{1}{2(b_1 + c_1)} \left(\frac{mK_{\Delta(\lambda)}bHu}{V} + R_{\Sigma} \right), & M_2 &= -\frac{m_3g}{(b_1 + c_1)}, \\ M_3 &= -\left(m_3g - 2F_3^e - \frac{K_{\Delta(\lambda)}bHu}{V} \right) \frac{(a_1 + b_1 + c_1)}{(b_1 + c_1)} \\ &\quad + \frac{P_u u c_1 \sin \chi}{\omega r_5 (b_1 + c_1)} + \frac{N_e d_1 \sin \beta}{\omega r_2 (b_1 + c_1)}, \\ N_1 &= \frac{1}{2(b_1 + c_1)} \left(\frac{mK_{\Delta(\lambda)}bHu}{V} + R_{\Sigma} \right), \\ N_2 &= \frac{r_3}{2(b_1 + c_1)} \left(\frac{mK_{\Delta(\lambda)}bHu}{V} + R_{\Sigma} \right), \\ N_3 &= \frac{P_u u b_1 \cos \chi}{\omega r_5 (b_1 + c_1)} + \frac{N_e (b_1 + c_1 + d_1) \cos \beta}{\omega r_2 (b_1 + c_1)}, \\ S_1 &= -\frac{1}{2(b_1 + c_1)} \left(\frac{mK_{\Delta(\lambda)}bHu}{V} + R_{\Sigma} \right), \\ S_2 &= -\frac{r_3}{2(b_1 + c_1)} \left(\frac{mK_{\Delta(\lambda)}bHu}{V} + R_{\Sigma} \right), \end{aligned}$$

$$S_3 = \frac{P_u u c_1 \cos \chi}{\omega r_5 (b_1 + c_1)} - \frac{N_e d_1 \cos \beta}{\omega r_2 (b_1 + c_1)}.$$

In the above expressions: $N_e = K_{\Delta(\lambda)} b H u + P_u u$, $F_3^e \approx 1.5 N_e / V$ [5, 6, 7].

2.4. Dynamic Reactions Depending on the Kinematics and Mass Characteristics of the Mechanical System

The dynamic reactions, depending on the kinematics and mass characteristics of the rotating body are shown in Fig. 8.

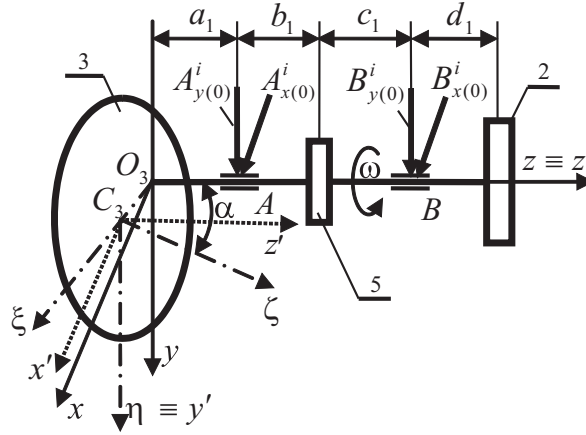


Fig. 8. Dynamic reactions caused by the kinematics and mass characteristics

We define them using formulas known in the literature [8, 9, 10]. We consider motion with constant angular velocity i.e. $\omega = \text{const}$, $\varepsilon = 0$, where ε is the angular acceleration of the mechanical system. In this case, the dynamic reactions are constant with respect to the moving coordinate system. These reactions change about the fixed coordinate system depending on the change in the angle φ . We can determine their sizes to an arbitrary position. Therefore, we choose the initial position when $\varphi = 0$. For this position, the axes of the fixed coordinate system O_3xyz and the moving coordinate system $O_3x_1y_1z_1$ coincide.

The expressions for these reactions are derived by the author [11]. They

have the following form towards the moving coordinate system $O_3x_1y_1z_1$:

$$\begin{aligned}
 A_{x(0)}^i &= -\frac{m_3\omega^2}{(b_1 + c_1)}(a_1 + b_1 + c_1 + e \sin \alpha)e \cos \alpha \\
 &\quad + \frac{\omega^2}{2(b_1 + c_1)}(J_\xi - J_\zeta) \sin 2\alpha, \\
 (25) \quad B_{x(0)}^i &= \frac{m_3\omega^2}{(b_1 + c_1)}(a_1 + e \sin \alpha)e \cos \alpha - \frac{\omega^2}{2(b_1 + c_1)}(J_\xi - J_\zeta) \sin 2\alpha, \\
 A_{y(0)}^i &= B_{y(0)}^i = 0.
 \end{aligned}$$

The following kinematics and mass characteristics are used in the above expressions: $A_{x(0)}^i$, $B_{x(0)}^i$, $A_{y(0)}^i$, $B_{y(0)}^i$ are the dynamic reactions, caused by the kinematics and mass characteristics of the mechanical system. The geometrical dimensions, shown in Fig. 8, are marked with a_1 , b_1 and c_1 . J_ξ and J_ζ are the mass moments of inertia of the feeding wheel 3 with respect to the axes ξ and ζ . They are calculated for each concrete case.

We write the final expressions received by the author [11] for the dynamic reactions A_x^i , B_x^i , A_y^i , B_y^i for an arbitrary position ($\varphi \neq 0$). These correlations show the change of the dynamic reactions toward the fixed coordinate system O_3xyz .

$$\begin{aligned}
 A_x^i &= \left[-\frac{m_3\omega^2}{(b_1 + c_1)}(a_1 + b_1 + c_1 + e \sin \alpha)e \cos \alpha \right. \\
 &\quad \left. + \frac{\omega^2}{2(b_1 + c_1)}(J_\xi - J_\zeta) \sin 2\alpha \right] \cos \omega t, \\
 A_y^i &= \left[-\frac{m_3\omega^2}{(b_1 + c_1)}(a_1 + b_1 + c_1 + e \sin \alpha)e \cos \alpha \right. \\
 &\quad \left. + \frac{\omega^2}{2(b_1 + c_1)}(J_\xi - J_\zeta) \sin 2\alpha \right] \sin \omega t, \\
 (26) \quad B_x^i &= \left[\frac{m_3\omega^2}{(b_1 + c_1)}(a_1 + e \sin \alpha)e \cos \alpha \right. \\
 &\quad \left. - \frac{\omega^2}{2(b_1 + c_1)}(J_\xi - J_\zeta) \sin 2\alpha \right] \cos \omega t, \\
 B_y^i &= \left[\frac{m_3\omega^2}{(b_1 + c_1)}(a_1 + e \sin \alpha)e \cos \alpha \right. \\
 &\quad \left. - \frac{\omega^2}{2(b_1 + c_1)}(J_\xi - J_\zeta) \sin 2\alpha \right] \sin \omega t.
 \end{aligned}$$

The full dynamic reactions at the supports A and B are sum of the dynamic reactions of the external loading and the dynamic reactions depending on the kinematics and the mass characteristics of the rotating body.

$$(27) \quad \begin{aligned} A_x &= A_x^e + A_x^i, & A_y &= A_y^e + A_y^i, \\ B_x &= B_x^e + B_x^i, & B_y &= B_y^e + B_y^i. \end{aligned}$$

We substitute expressions (24) and (26) into the above expressions to obtain the full expression for the dynamic reactions A_x, A_y, B_x, B_y .

$$\begin{aligned} A_x &= S_1 e \cos \alpha \cos \omega t + S_2 \cos \alpha + S_3 - \\ &\quad - \frac{\omega^2}{(b_1 + c_1)} \left[m_3(a_1 + b_1 + c_1 + e \sin \alpha) e \cos \alpha - \frac{1}{2} (J_\xi - J_\zeta) \sin 2\alpha \right] \cos \omega t, \end{aligned}$$

$$\begin{aligned} A_y &= M_1 e \cos \alpha \sin \omega t + M_2 e \sin \alpha + M_3 - \\ &\quad - \frac{\omega^2}{(b_1 + c_1)} \left[m_3(a_1 + b_1 + c_1 + e \sin \alpha) e \cos \alpha - \frac{1}{2} (J_\xi - J_\zeta) \sin 2\alpha \right] \sin \omega t, \end{aligned} \quad (28)$$

$$\begin{aligned} B_x &= N_1 e \cos \alpha \cos \omega t + N_2 \cos \alpha + N_3 + \\ &\quad + \frac{\omega^2}{(b_1 + c_1)} \left[m_3(a_1 + e \sin \alpha) e \cos \alpha - \frac{1}{2} (J_\xi - J_\zeta) \sin 2\alpha \right] \cos \omega t, \end{aligned}$$

$$\begin{aligned} B_y &= L_1 e \cos \alpha \sin \omega t + L_2 e \sin \alpha + L_3 + \\ &\quad + \frac{\omega^2}{(b_1 + c_1)} \left[m_3(a_1 + e \sin \alpha) e \cos \alpha - \frac{1}{2} (J_\xi - J_\zeta) \sin 2\alpha \right] \sin \omega t. \end{aligned}$$

3. Numerical example

The results of the carried out computer experiments are presented in Figs 9 and 10. We use the following initial data [1, 12, 13]: $\omega = 56$ [s⁻¹], $e = 0.001$ [m], $\alpha = 0.017$ [rad], $a_1 = 0.25$ [m], $b_1 = 0.45$ [m], $c_1 = 0.45$ [m], $d_1 = 0.35$ [m], $m_3 = 810$ [kg], $J_\xi = 171$ [kg m²], $J_\zeta = 336$ [kg m²], $N_e = 43.4$ [kW], $V = 45$ [m/s], $r_1 = 0.12$ [m], $r_2 = 0.25$ [m], $r_3 = r_4 = 0.8$ [m], $r_5 = 0.1$

[m], $r_6 = 0.16$ [m], $i_{12} = 2.08$, $\omega_e \leq 117.56$ [s⁻¹], $s = 1.47$ [mm], $b = 2.5$ [mm], $\alpha_\rho = 2.5$, $p_3 = 9220$ [N/m], $k = 35 \times 10^6$ [Pa], $\alpha_\lambda = 245 \times 10^3$ [Pa], $\alpha_\Delta = 196 \times 10^3$ [Pa], $m = 0.5 \div 1$, $H = 0.42$ [m], $u = 0.5$ [m/s], $u_z = 2.5$ [mm], $K_\Delta = 80 \times 10^6$ [J/m³], $\beta = 0.2$ [rad], $\gamma = 0.1$ [rad], $R_3^e = 1425$ [N], $P_3^e = 930$ [N], $F_3^e = 1450$ [N], $R_\Sigma = 2400$ [N], $P_u = 2850$ [N].

Figure 9 shows the diagrams of the dynamic reactions A_x , B_x , A_y , B_y .

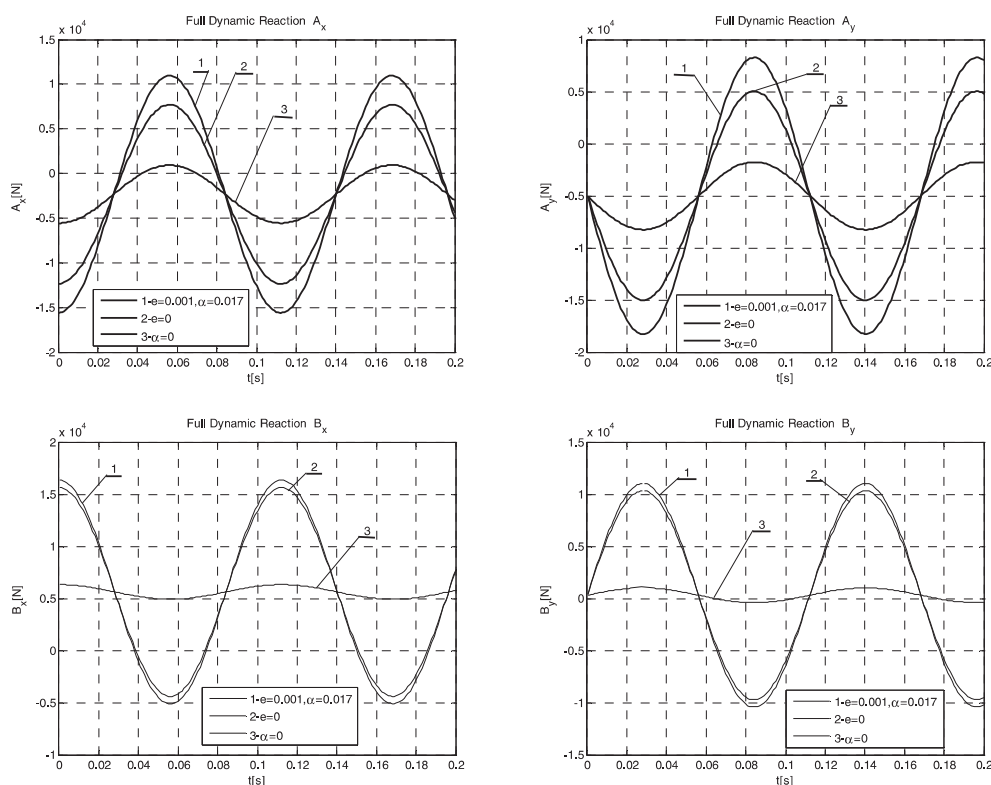


Fig. 9. Dynamic reactions A_x , A_y , B_x , B_y

These diagrams show the dependence of the dynamic reactions A_x , B_x , A_y , B_y from the time t on given values of the eccentricity e and the angle α . The diagrams, marked with 1 are drawn in a case where $e = 0.001$ [m] and $\alpha = 0.017$ [rad]. The diagrams, marked with 2 are drawn in a case where no eccentricity, i.e. $e = 0$. The diagrams, marked with 3 are drawn in a case when the angle α is equal to zero, i.e. $\alpha = 0$. The bearing load is maximum when $e \neq 0$ and $\alpha \neq 0$ and a minimum when $\alpha = 0$. Obviously, the angle α has a greater influence on the size of the dynamic reactions than the eccentricity e .

Figure 10 shows the amplitude values of the dynamic reactions:

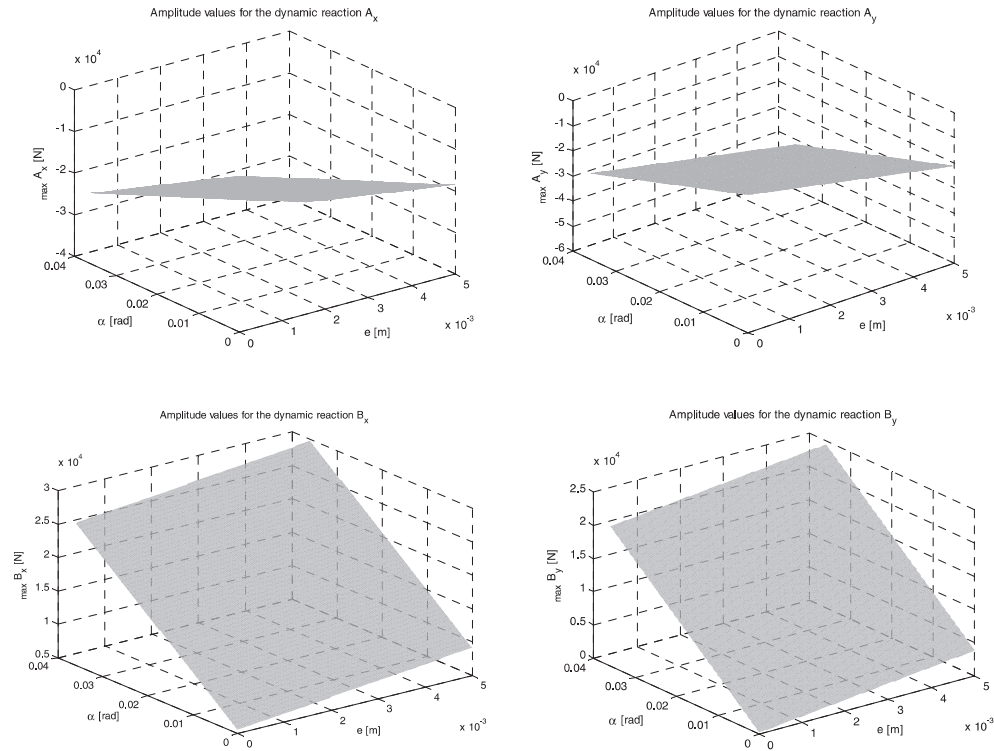


Fig. 10. Amplitude values of the dynamic reactions A_x , B_x , A_y , B_y

These diagrams show the dependence of the amplitude values on the dynamic reactions A_x , B_x , A_y , B_y from the eccentricity e and the angle α . We can determine the amplitude values of the dynamic reactions for each value of the eccentricity e and the angle α . Thus, we can determine the most favourable operating mode of band saw machine. Obviously, the diagrams show that the dynamic reactions at the supports are different at equal values of e and α . This fact should be taken into account in determining the optimum operating conditions for the mechanical system.

4. Conclusion

In the proposed work, the dynamic processes in the band saw machines are analyzed. Dynamic forces arise as a result of these processes. Dynamic reactions are generated in the bearing A and B . These reactions are caused by the external loads and the kinematics and the mass characteristics of the

mechanical system (the feeding wheel 3, the belt pulleys 2 and 5 and the basic shaft). This fact allows obtaining expressions for the calculation of the full dynamic reactions. Computer calculations are carried out and the diagrams are drawn. We can establish the conditions in which loading of the bearings possess minimum values from the analysis of the final expressions.

In conclusion we can say that the derived results can be used to guarantee normal work of the band saw machines in normal operation. This study can be used as a basis for future works and modelling of the dynamic processes so that the dynamic reactions to have minimum values.

REFERENCES

- [1] GOCHEV, G. Handbook for Exercise of Wood Cutting and Woodworking Tools, Sofia, Publishing House in LTU, 2005 (in Bulgarian).
- [2] FILIPOV, G. Woodworking Machines, Sofia, Technics, 1977 (in Bulgarian).
- [3] GENCHEV, G., P. OBRESHKOV. Projection and Trial of Woodworking Machines, Sofia, 1998 (in Bulgarian).
- [4] MAKOVSKIJ, N. V. Theory and Constructions of Woodworking Machines, Moscow, Forest Industry, 1984 (in Russian).
- [5] OBRESHKOV, P. Woodworking Machines, Sofia, Publishing house "B M", 1995 (in Bulgarian).
- [6] WALKER, J. C. F. Primary Wood Processing: Principles and Practice, London, Chapman&Hall, 1993.
- [7] GOCHEV, G. Forces and Cutting Power in Cutting up of a Beech Wood with Scored Band Saw with a Roller Feeding. *Journal of "Wood and Furniture"*, No. 2 (2002), No. 1 (2003), Sofia, 19–21 (in Bulgarian).
- [8] KISYOV, I. Handbook of the Engineer, Part One- Mathematics, Sofia, Technical Press, 1979 (in Bulgarian).
- [9] KISYOV, I. Handbook of the Engineer, Part Two – Mechanics, Sofia, Technical Press, 1979 (in Bulgarian).
- [10] MARINOV, B. Dynamic Reactions in the Bearings of Circular Shafts, Driving Big Circular Saws. *Journal of Mechanics of Machines*, Varna, **68** (2007), No. 2, 119–123.
- [11] MARINOV, B. Dynamic Reactions in the Basic Shaft Bearings of Band Saw Machines. *Journal of Mechanics of Machines*, Varna, **100** (2013), No. 1, 81–86.
- [12] FRONIUS, K. The Saw Filer. A Practical Guide to Tool Maintenance in Saw and Planing Mills, Biberach, Vollmer Werke, 1999.
- [13] BRUCE, R. Understanding Wood. A Craftsman's Guide to Wood Technology, Newtown, Connecticut, Taunton Press, 1995.

- [14] KAZAKOFF, A. Force Response Transmissibility Prediction and Frequency Analysis of High Deflection Displacement Magnitudes. *Journal of Theoretical and Applied Mechanics*, **37** (2007), No. 3, 3–18.
- [15] KAZAKOFF, A. A Study of the Influence of the Belt Kinematic Pair on the Spatial Vibrations of a Single Mass Model, VIth National Congress on Theoretical and Applied Mechanics, Bulgaria, Varna, 1989, 121–127.
- [16] KAZAKOFF, A., Z. TCHERNEVA-POPOVA, P. PARUSHEFF. Mechano Mathematical Models for Mechatronic Systems For Vibration Jaw Crushing Processes. *Journal of Mechanism and Machine Theory*, **29** (1994), No. 8, 1167–1178.
- [17] RONGONG, J., A. KAZAKOFF. Computer Modelling of the Dynamic Response of Viscoelastic Vibroisolators. *Journal of Engineering Mechanics*, Brno, Check Republic, **13** (2006), No. 1, 19–30.